DOI: 10.1021/ma1013644

Macromolecules
ARTICLE

Origin of High Segmental Mobility at Chain Ends of Polystyrene

Yohei Miwa,*,† Shigetaka Shimada,‡ Osamu Urakawa,§ and Shogo Nobukawa§

†*Analytical Technology Laboratory, R & D Center, Mitsubishi Chemical Corpolation, 1, Toho-cho, Yokkaichi, Mie 510-8530, Japan,* ‡*Depaertment of Materials Science and Technology, Nagoya Institute of Technology, Gokiso-cho, Showa-ku, Nagoya 466-8555, Japan, and* §*Department of Macromolecular Science, Graduate School of Science, Osaka University, 1-1 Machikaneyama, Toyonaka, Osaka 560-0043, Japan*

Received June 20, 2010; Revised Manuscript Received July 23, 2010

ABSTRACT: Effects of solvents on segmental dynamics of polystyrene (PS) at the chain end have been studied by the site-specific spin-label method of electron spin resonance (ESR). PS's having similar number-average molecular weight (ca. 25 kDa) but labeled with a nitroxde at the chain end (E-PS) or midchain segments (M-PS) individually were used for the measurements. Toluene and dioctyl phthalate (DOP) which are good and theta solvents, respectively, for PS were selected as solvents. The temperature variation of ESR spectra was simulated based on the "macroscopic order with microscopic disorder" model to determine the segmental mobility of the labeled segment. The E-PS showed obviously and slightly higher mobility compared to the M-PS in the bulk PS and in the concentrated PS/DOP (50/50) solution, respectively. On the other hand, the E-PS showed the same mobility with the M-PS within experimental uncertainties in the dilute PS/toluene (1/99), concentrated PS/toluene (60/40), and dilute PS/DOP (3/97) solutions. Namely, the chain end showed higher segmental mobility than midchain segments in high viscous media where large intermolecular hindrances such as frictional resistance, spatial restriction for conformational transition, and intermolecular coupling are expected. From this result, we conclude that lesser intermolecular hindrances around chain ends are the origin of the higher mobility at the chain end segments.

Introduction

Almost every polymer has chain ends, and they play important roles in the polymer physics. It is widely and nebulously believed that chain ends of a polymer have higher mobility compared to the midchain segments. For instance, a depression of the glass transition temperature (T_g) with decreasing the molecular weight is attributed to an increase in the chain end concentration.[1,2] Furthermore, Kajiyama and co-workers interpreted that the aggregation of chain ends at the surface of a polystyrene (PS) film was one of the causes of the depression in T_g at the surface of the film.[3] Nevertheless, the dynamic properties of the chain end have not been perfectly clear yet. For example, do chain ends maintain higher mobility when the concentration of polymer is varied from the bulk state to the dilute solution? In the bulk the frictional resistance and motional coupling between polymer segments are significant, whereas the polymer−polymer interaction is almost canceled, but the interaction with the solvent is generated in the dilute solution with good solvents. Therefore, the difference in mobility at the chain end and middle segments is probably different in these conditions. This topic is interesting to reveal the origin of the higher segmental mobility at the chain ends. The present work is the first study focusing on this topic.

Generally speaking, it is difficult to pick up experimentally the information focused on the chain end. For this problem, label techniques are very powerful, and various label techniques, such as photolabeling,[4,5] deuterium-labeling,[6] dielectric-labeling,[7] and spin-labeling,[8−14] have been applied to determine the motional and structural properties of chain ends.

Previously, our group showed that chain ends of PS, poly(methyl methacrylate), poly(cyclohexyl acylate) (PCHA), and poly(cyclohexyl methacrylate) have higher segmental mobility compared to the midchain segments *in the bulk states* using the site-specific spin-label method of electron spin resonance (ESR).[13−16] In these works, the chain end or midchain segments were selectively labeled with a stable nitroxide radical; the mobility of the spin-labels was determined from change in the spectral shape with a variation of temperature. Because the spectral shape is insensitive for motion on time scale slower than 10^{-7} s,[17] the measurement temperature is typically more than $T_g + 50$ K. On the other hand, the author recently developed a novel method for the detection of the T_g of the spin-labeled polymer applying a microwave power saturation of ESR.[18] Using this method, it was shown that the T_g of PCHA labeled at the chain end was very slightly, a few kelvin, lower than that of the one labeled at the midchain segments. Very recently, Lund et al. studied the chain end mobility of end-functionalized oligomer PS (M_n = 2.2 kDa) over an extensive temperature range (ca. 110−413 K) using dielectric spectroscopy.[7] They observed the higher mobility of chain ends; this is in good agreement with our ESR results. The higher mobility around chain ends *at the glass transition* in the bulk state can be rationalized in the free volume, the entropy, and the coupling models by the chain ends having respectively excess free volume,[2] excess configurational entropy,[19] and deficient intermolecular constraints.[20] The larger free volume around chain ends were detected by various experiments such as photolabel method,[4] positron annihilation lifetime technique,[21] and dilatometric measurement.[22] The chain end showed unique behavior in the diffusion motion, too. Welp et al. compared the diffusion behaviors of central and end sections of a PS chain during welding of films using specular neutron reflectivity with a deuterium-label method.[6] The diffusion behaviors of each segment were monitored directly via deuterium depth profiles; it was revealed that the diffusion of the chain end section was faster than that of the center section during welding. The reptation model was necessary to explain the diffusion behavior of the center section while the diffusion

*To whom correspondence should be addressed. E-mail: 7804052@cc.m-kagaku.co.jp.

 Published on Web 08/03/2010

behavior of the chain end section was interpreted by the Rouse model. This result clearly indicates that the higher diffusion motion at the chain end section is due to lesser entanglements compared to the center section.

In the solution, several ESR studies on polymer chain end mobility were carried out using the spin-label method, and the correlation time and activation energies for the chain end were compared with those for the chain center and the phenyl ring.[8−12] At 298 K, the correlation time determined from the analysis of the line width of ESR spectrum for the end-labeled PS in toluene was about 2.4×10^{-10} s, whereas that for the PS labeled at the phenyl ring was about 5.9×10^{-10} s. They also differ in activation energies, that is, 5.8 and 9.0 kJmol^{-1} for end-labeled and ring-labeled PS, respectively.[9] Namely, the higher mobility of chain ends in the solution was suggested. However, it should be noted that the correlation time determined from the analysis of the line width of ESR spectrum is including a contribution of the rotation around polymer−label bond which is usually faster than the diffusion motion of the labels; therefore, contributions of the rapid rotation around the polymer−label bond could be included in the experimental results.[8−10] Horinaka et al. compared the mobility of the chain end and the center of the PS main chain using the fluorescence depolarization method from 283 to 303 K.[5] In this study, the anthracene molecule was bonded at the end or the center of the PS main chain. As the molecular weight of the PS was more than 2 kDa, the correlation time for the end-labeled PS in benzene at 293 K was about 3.0×10^{-10} s, whereas that for the center chain one was about 2.0×10^{-9} s. They concluded that the conformational transition at the chain end occurs easily compared to the center of the chain. On the other hand, the difference in the activation energy between the chain end (ca. 6.3 kJ mol^{-1}) and the chain center (ca. 7.1 kJ mol^{-1}) was not so marked as compared to the difference in the correlation time. Therefore, they assumed that the activation energy was mainly determined by the size of the label attached to the main chain.

In summary, the previous works basically proposed that the chain ends have distinctly higher mobility compared to the midchain segments irrespective of the environment surrounding the polymer segments. In the present study, the mobility at the chain end and midchain segments of PS are compared in the dilute solution, concentrated solution, and the bulk using the site-specific spin-label method to reveal the effect of the local concentration around the PS segments on the mobility of chain ends. Toluene and dioctyl phthalate (DOP) were selected as solvents because toluene is low viscous and good solvent for PS while DOP is high viscous and theta solvent for PS (the theta temperature is around 295 K).[23] The same spin-labeling was carried out for the chain end and midchain segments; the ESR spectra were analyzed by the computer simulation to exclude the contribution of the rotation at the polymer−label bond.

Experiments

Sample Preparation. Two PS's having the same molecular weight but labeled at different sites, the chain end or the midchain, with a nitroxide via a short tether were prepared (Chart 1). The notations for the end-labeled and midchain-labeled PS's are defined to be E-PS and M-PS, respectively. Synthesis of the E-PS and M-PS was described in elsewhere.[13] The number-average molecular weight (M_n) and the molecular weight distribution (M_w/M_n) for the E-PS determined by gel permeation chromatography (GPC) were 26.1 kDa and 1.09, respectively. On the other hand, the M_n and M_w/M_n for the M-PS were 24.9 kDa and 1.15, respectively. Solvents used in measurements were toluene (Kishida Chemical Co., Ltd., Extra Pure Reagent) and dioctyl phthalate (DOP, Nacalai Tesque, Extra Pure Reagent). Before use, the solvents were dried with molecular sieves (3A). In preparing the sample solution, the PS and solvents were stirred in a bottle until the solution becomes homogeneous. The solution was transferred into a 5 mm o.d. quartz tube for the ESR measurement using a syringe; the tube was sealed under a nitrogen gas following the degasification by the freeze−pump−thaw method.

Chart 1

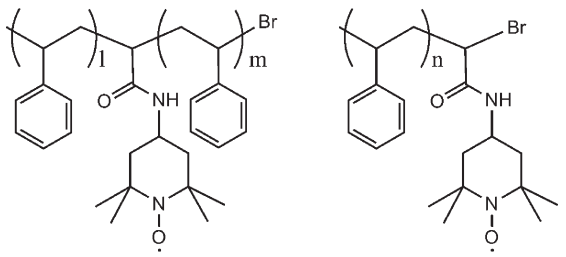

M-PS E-PS

Measurements. ESR spectra were recorded with JEOL X-band FA300 spectrometers with 100 kHz field modulation. The temperature was controlled within ±0.1 K. All samples were allowed to equilibrate for at least 5 min after reaching the desired temperature. The magnetic field and g tensor were calibrated with Mn^{2+}. Most spectra were collected with the following parameters: sweep width 150 G, microwave power 0.1 mW, time constant 30 ms, 2−4 scans, and 2048 points. The modulation amplitude was varied in the range 0.2−2 G, depending on the line width. The microwave power was controlled to avoid the saturation.

GPC was carried out with following condition: in THF (1 mL/min) at 313 K on four polystyrene gel columns (Tosoh TSK gel GMH (beads size is 7 μm), G4000H, G2000H, and G1000H (5 μm)) that were connected to a Tosoh CCPE (Tosoh) pump and an ERC-7522 RI refractive index detector (ERMA Inc.). The columns were calibrated against standard PS (Tosoh) samples.

Simulation of ESR Spectra. ESR spectra were calculated with the software based on the stochastic Liouville equation,[24] as described previously.[25] Simulated spectra were fitted to experimental spectra using a PC version of the NLSL program based on the modified Levenberg−Marquart minimization algorithm, which iterates the simulations until a minimum least-squares fit to experiment was reached.[26] The g and ^{14}N hyperfine (A) tensors were determined by analyzing rigid-limit spectra measured at 77 K.

The model known as "microscopic order with macroscopic disorder" (MOMD) was applied for calculating the spin-label rotational diffusion.[27] The model assumes that the spin-labels undergo microscopic molecular ordering with respect to a local director; the local directors in the sample are randomly oriented in the laboratory frame. Interpretations for the parameters used in this simulation model were given in detail in ref 27d. Pilař has summarized the successful application of the MOMD model for analyzing ESR line shapes of spin-labeled polymers.[28] The rotational diffusion of nitroxide spin-labels attached to polymer chain segments has been approximated by superposition of the isotropic rotational diffusion of the polymer chain segment with the rotational diffusion coefficient, R_S, and the internal rotation at the tether bond of the spin-label with the rotational diffusion coefficient, R_I.[28] When the nitroxide spin-label is attached to a polymer chain via a short tether, it is assumed that $R_{prp} = R_S$ and $R_{pll} = R_I + R_S$. Here, R_{pll} and R_{prp} are the parallel and perpendicular rotational diffusion coefficients against the tether bonds of the nitroxide to the polymer backbone, respectively. In addition, the axis of internal rotation can be tilted relative to the z-axis of the nitroxide axis system and specified by angle β. Here, the z-axis of the nitroxide axis system is parallel to the axis of the nitrogen p-orbital. The spin-label used in this work is the same with that used by Pilař et al., and the β is illustrated on page 141 in ref 28. The tether involves three single bonds (C−CO,

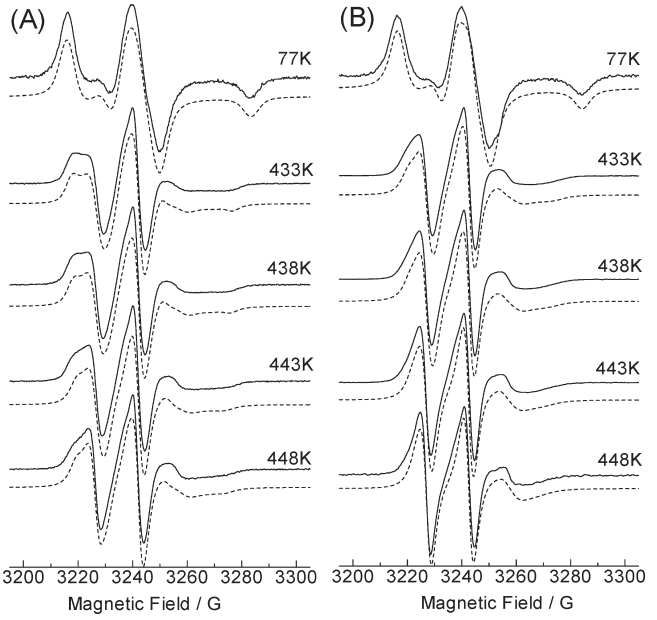

Figure 1. Experimental and fitted ESR spectra for M-PS (A) and E-PS (B) in the bulk. Experimental and fitted spectra are shown with solid and dotted lines, respectively.

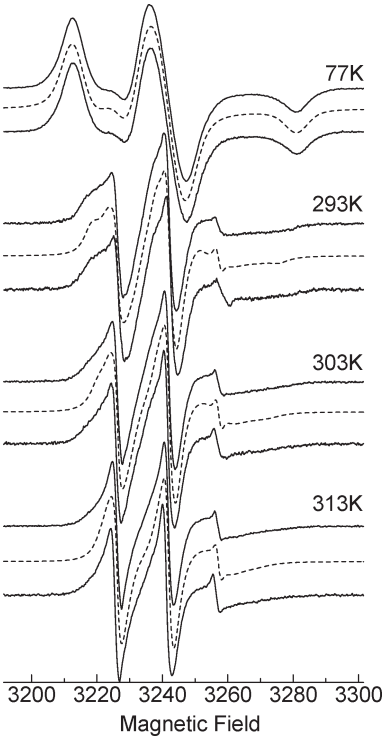

Figure 2. Experimental and fitted ESR spectra for M-PS and E-PS in concentrated PS/toluene (60/40) solution. Experimental spectra for M-PS and E-PS are shown at the top and the bottom at each temperature, respectively. Fitted spectra for M-PS are shown with dotted line.

CO−NH, and NH−SL). The second one, a peptide bond, is normally fixed, and it is expected that the free rotation is restricted for the first bond because of the steric constraint. Therefore, the only bond which rotates freely is the third bond, NH−SL.

Results

Selected experimental and fitted ESR spectra of M-PS and E-PS in the bulk, concentrated PS/toluene (60/40) solution, dilute

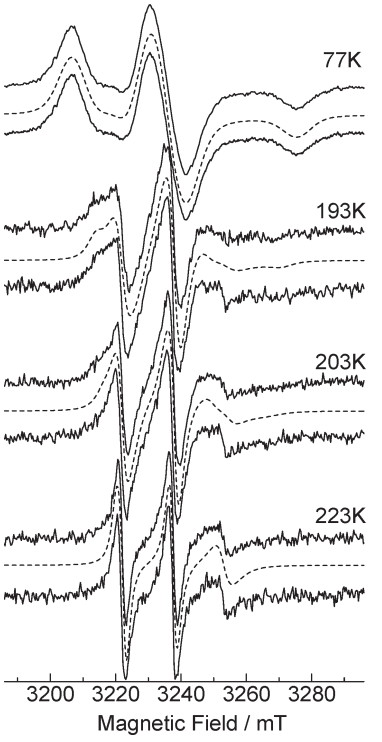

Figure 3. Experimental and fitted ESR spectra for M-PS and E-PS in dilute PS/toluene (1/99) solution. Experimental spectra for M-PS and E-PS are shown at the top and the bottom at each temperature, respectively. Fitted spectra for M-PS are shown with dotted line.

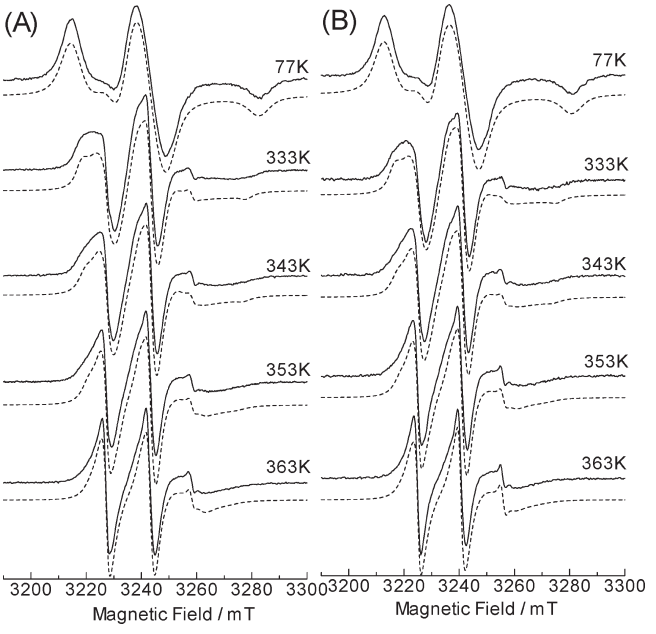

Figure 4. Experimental and fitted ESR spectra for M-PS (A) and E-PS (B) in concentrated PS/DOP (50/50) solution. Experimental and fitted spectra are shown with solid and dotted lines, respectively.

PS/toluene (1/99) solution, concentrated PS/DOP (50/50) solution, and dilute PS/DOP (3/97) solution in the range 77−448 K are shown in Figure 1, 2, 3, 4, and 5, respectively. Each spectrum was vertically shifted to avoid overlapping. The temperature dependence of the ESR line shape is due to changes in the rotational rate of the nitroxide radical with correlation time, τ_c, defined as $(6(R_{prp}{}^2 R_{pll})^{1/3})^{-1}$. In the bulk and the concentrated PS/DOP (50/50) solution, the E-PS and M-PS showed different

Table 1

sample	g_{xx}	g_{yy}	g_{zz}	A_{xx}/G	A_{yy}/G	A_{zz}/G	E_S/kJ mol^{-1}	E_I/kJ mol^{-1}
bulk, M-PS	2.0099	2.0065	2.0025	7.04	5.02	33.6	126	44
bulk, E-PS	2.0100	2.0064	2.0025	7.04	5.02	34.0	103	42
PS/toluene (1/99), M-PS	2.0100	2.0064	2.0025	6.80	5.08	34.4	18	12
PS/toluene (60/40), M-PS	2.0100	2.0064	2.0025	7.19	5.00	34.2	53	16
PS/DOP (3/97), M-PS	2.0100	2.0064	2.0027	7.00	5.10	34.2	45	28
PS/DOP (50/50), M-PS	2.0099	2.0065	2.0027	7.19	5.05	34.1	75	28
PS/DOP (50/50), E-PS	2.0100	2.0063	2.0027	7.32	4.95	34.0	71	26

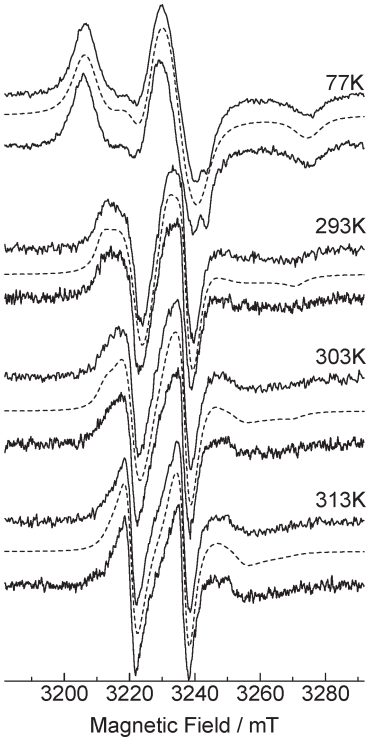

Figure 5. Experimental and fitted ESR spectra for M-PS and E-PS in dilute PS/DOP (3/97) solution. Experimental spectra for M-PS and E-PS are shown at the top and the bottom at each temperature, respectively. Fitted spectra for M-PS are shown with dotted line.

ESR spectra at the same temperature; therefore, the fittings were carried out for each spectrum separately. On the other hand, the experimental spectra of the E-PS and M-PS in the concentrated PS/toluene (60/40) solution, the dilute PS/toluene (1/99) solution, and the dilute PS/DOP (3/97) solution were shown together with the fitted one for the M-PS at each temperature because the E-PS and M-PS showed the similar spectral shape within experimental uncertainties. That indicates that the mobilities of the chain end and midchain segment are comparable in these solutions.

The rigid-limit spectra observed at 77 K were successfully fitted using the NLSL program with very slow isotropic Brownian rotational diffusion of the spin-label (log R_{pll} = log R_{prp} = 3). Best fits required a superposition of Lorentzian line shapes with Gaussian inhomogeneous broadening. The A and g tensors used for the best fits are listed in Table 1. These tensors were fixed for the fitting of the temperature-dependent ESR spectra. On the other hand, the parameters R_S and R_I and the other parameters describing the local dynamics in PS chains were temperature-dependent and determined by fitting experimental spectra. ESR spectra of samples were basically fitted with a single spectral component. However, very small amount (only a few percent) of an additional spectral component which was much faster than the major component was observed for some experimental spectra of the solution samples. This additional component could not be removed by the further purification of the spin-labeled PS. Moreover, the intensity of the additional component increased after 1 day. Therefore, it is expected that there is a slow detachment of some of the spin-labels; as a result, free label agent was generated in the solution. The same phenomenon was reported by Pilař et al.[28] Such spectra have been analyzed using two-site models. For the additional component, a simple axially symmetric Brownian rotational diffusion and practically the same values for A and g tensor components as for the major component were applied.

Arrhenius plots of R_S and R_I (rotational diffusion coefficient for the polymer chain segment and the internal rotation of the spin-label at the tether bond, respectively) for the bulk, the PS/toluene solutions, and the PS/DOP solutions are shown in parts A, B, and C of Figure 6, respectively, and the corresponding activation energies E_S and E_I are listed in Table 1. The tilt angles β are almost constant (63 ± 3°). This value agrees well with the orientation of the NH−C, which is expected to be the only bond contributing to the internal rotation of the spin-label with respect to the polymer chain segment, estimated from the crystal structure of the bis(2,2,6,6-tetramethyl-4-piperidinyl-1-oxy) substrate.[29] The parameter c_0^2 characterizes the component of the ordering potential symmetric in the plane perpendicular to the direction of the preferred rotational tensor symmetry axis orientation specified by the angle β. The parameter c_2^2 characterizes rhombic distortion of the ordering potential. The ordering potentials characterized by the parameters are illustrated in Figure 8 in ref 27d in detail. These parameters decreased with increasing temperature.

The T_{ref} which is defined as temperature at log R_S = 6.5 for each samples was plotted against the concentration of the PS in Figure 7. For both the PS/toluene and PS/DOP solutions, the T_{ref} increased with increasing the concentration of the PS because of the increase in the viscosity of the solutions. Moreover, the T_{ref} in the PS/DOP solution showed larger value compared to the PS/toluene solution because of the higher viscosity of the DOP. The difference in the T_{ref} for the E-PS and M-PS was the most significant for the bulk state; the difference decreased with decreasing the viscosity of the system.

Discussion

Influence of Spin-Labeling on the Segmental Motion of PS. Labeling methods are excellent to highlight the local motion of polymers; however, there is a possibility of that the labeling agents disturb the original segmental motion of the polymer. In this section, the mobility determined by the spin-label method is compared with that determined by other techniques, and we discuss the influence of the spin-labeling.

Ediger and co-workers determined the segmental correlation time ($\tau_{seg,NMR}$) of three PS (M_n = 1.6, 2.1, and 10.9 kDa) taken from NMR by measuring the ^{2}H spin−lattice relaxation times over a broad temperature range (390−510 K).[30] The $\tau_{seg,NMR}$ for the PS (M_n = 10.9 kDa) referred from ref 30 was converted to R and plotted in Figure 6A. The NMR data was in excellent agreement with the R_S of the M-PS. From this result, the disturbance of the spin-labeling is little for the bulk PS. According to the modern concept of

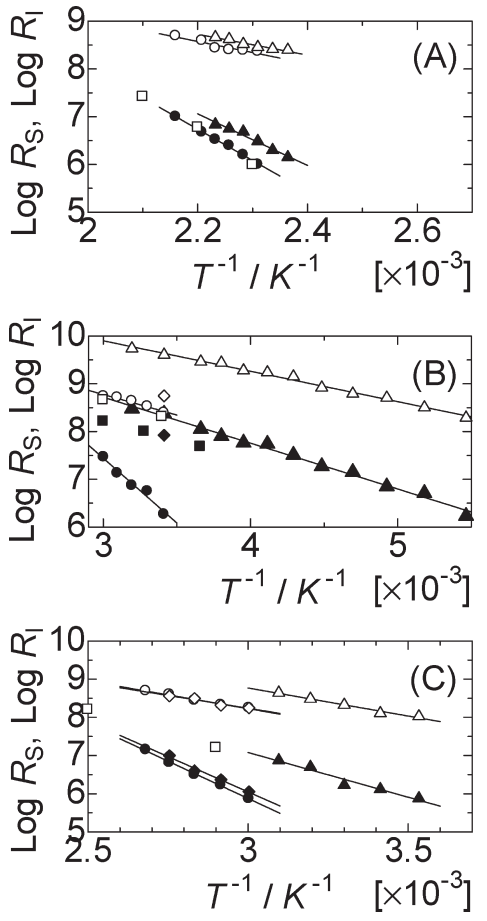

Figure 6. Arrhenius plots of rotational diffusion coefficients R_S and R_I in bulk PS (A), PS/toluene solutions (B), and PS/DOP solutions (C). (A) Solid and open circles represent R_S and R_I for M-PS, respectively. On the other hand, R_S and R_I for E-PS are shown with solid and open triangles, respectively. Open square is NMR data for bulk PS (M_n = 10.9K) referred from ref 30. (B) Solid and open circles represent R_S and R_I for concentrated M-PS/toluene (60/40) solution, respectively. Solid and open triangles represent R_S and R_I for dilute M-PS/toluene (1/99) solution, respectively. Open square is NMR data for dilute PS/toluene solution taken from ref 31. Fluorescence data for PS labeled with anthracene at the center of chain in 2-butane taken from ref 32 are shown with solid square. Similarly, fluorescence data for PS labeled with anthracene at the center and end of chain in benzene taken from ref 5 are shown with solid and open diamonds, respectively. (C) Solid and open triangles represent R_S and R_I for dilute M-PS/DOP (3/97) solution, respectively. For concentrated PS/DOP (50/50) solution, solid and open circles represent R_S and R_I for M-PS, respectively, while solid and open diamonds represent R_S and R_I for E-PS, respectively. Open square is NMR data for dilute PS/DOP solution referred from ref 31.

cooperative segmental relaxation, a polymer segment relaxes cooperatively with neighboring segments in the bulk.[31] Therefore, we predict that the original mobility of the spin-labeled segment is not far different from that of other PS segments; moreover, the difference in mobility between the PS and spin-labeled segments decreased because of the cooperative motion with neighboring segments.

The segmental dynamics of PS in various dilute solutions has been determined using NMR[30,31] and fluorescence depolarization.[5,32] For NMR measurement, the backbone was deuterated and the $\tau_{seg,NMR}$ was determined by the same method described above. On the other hand, the segmental correlation time from the fluorescence measurement ($\tau_{seg,fluo}$) is determined from monitoring the anthracene reorientation which is covalently bonded into the center or end of the chain backbone. The NMR data referred from ref 31 are plotted in

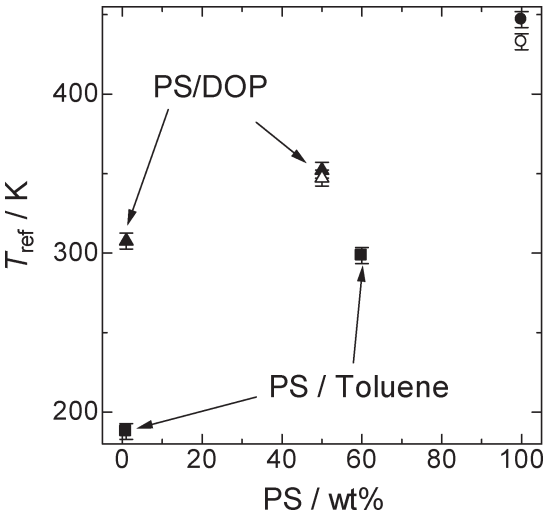

Figure 7. Plots of T_{ref} against concentration of PS. Circle, square, and triangle symbols are for the bulk PS, PS/toluene, and PS/DOP, respectively. Solid and open symbols are for M-PS and E-PS, respectively. Only solid symbol is shown for dilute PS/toluene (1/99), concentrated PS/toluene (60/40), and dilute PS/DOP (50/50) solutions because no difference in temperature-dependent ESR spectra was observed for M-PS and E-PS.

Figure 6B,C. For the fluorescence measurement, the data for the center-labeled and end-labeled PS taken from refs 5 and 32 are plotted in Figure 6B. The R_S determined by the ESR spin-labeling was in good agreement with the NMR data in the dilute PS/toluene and PS/DOP solutions whereas the mobility determined by the fluorescence measurement for the center-labeled one was significantly slower than that determined by the ESR and NMR. On the other hand, the fluorescence measurement for the end-labeled PS showed higher mobility than the ESR and NMR data. We will discuss about the fluorescence data for the end-labeled PS later. The difference in the mobilities determined by the NMR and fluorescence was discussed by Ediger et al.[33] They concluded that the PS segment around the anthracene became locally rigid and the length scale of the segmental motion detected in the fluorescence measurement is somewhat larger than that in the NMR measurements due to the introduction of the bulky anthracene chromophore into the PS backbone. We predict that the disturbance of the spin-labeling on the segmental motion of PS is negligible because the size of the spin-label agent is smaller than the anthracene, and the label is introduced as a side chain. Moreover, Pilař et al. also verified the little disturbance of the spin-labeling on the segmental mobility of PS in solutions by measuring the activation energies of the segmental motion of PS in various solvents having different viscosities.[28]

Effect of Local Concentration on Mobility at Chain End of PS. *In the Case of Bulk State*. The E-PS showed remarkably larger log R_S and smaller E_S compared to the M-PS in the bulk (see Figure 1, Figure 6A, and Table 1). This result is in good agreement with our previous result.[13] In the bulk, intermolecular hindrances such as frictional resistance, spatial restriction for conformational transition, and intermolecular coupling for segmental motion are significant. As pointed out by Fox and Flory, a larger specific free volume around a chain end is expected in the bulk because of the loose filling of polymer segments around chain ends.[1,2] The larger free volume around chain ends below T_g were shown by the photolabel method.[4] Since chain ends have larger specific free volume compared to midchain segments, the intermolecular hindrances around chain ends are expected to

be smaller. We consider that this is the origin of the higher segmental mobility of chain ends in the bulky polymer liquid.

Santangelo et al. reported that the fragility index of PS decreased with the reduction of the M_n.[34] They concluded that any conformational freedom conferred from chain ends reduced the fragility index. On the other hand, the fragility index of poly(dimethylsiloxane) (PDMS) was nearly M_n-independent because the ether linkage in the PDMS backbone gave nearly free rotation.[35] From these results, Rizos and Ngai pointed out that the difference in mobility between chain end and midchain segment is expected to be larger for polymers that have greater intermolecular coupling or large "fragility" because greater intermolecular cooperativity results in much lower mobility of the midchain segments.[20] In fact, the T_g of high-T_g polymers is generally more sensitive to the molecular weight (or the chain end fraction).[36,37] These results might predict that the difference in mobility between chain ends and midchain segments reduces when polymers are plasticized by additions of solvents.

In the Cases of Solutions. As shown in Figure 7, the T_{ref} decreased with an increase in the concentration of the solvent and the decrease was more significant for toluene than DOP due to the lower viscosity of toluene. This result indicates that the scale of the segmental motion of PS detected by the spin-labeling is influenced by the solvents. Chung et al. first proposed that the segmental mobility of a polymer in the miscible systems is determined by the "local concentration" around the segments.[38] Moreover, Lodge and McLeish proposed a model taking into account the "self concentration" of the polymer segment to determine the "local concentration" in the miscible polymer blends and solutions.[39] In this model, it is considered that the local concentration (ϕ_{eff}) of polymer is higher than the bulk concentration (ϕ) because of the chain connection. According to this model, the ϕ_{eff} is calculated by considering the ϕ and the self-concentration (ϕ_{self}):

$$\phi_{eff} = \phi_{self} + (1 - \phi_{self})\phi \quad (1)$$

Previously, we showed that the segmental dynamics of spin-labeled polymers in miscible polymer blends were reasonably predicted by the ϕ_{eff} calculated by this model.[15,16] Lutz et al. determined that the ϕ_{self} of PS segments in the toluene and DOP solutions to 0.19 ± 0.05 and 0.45 ± 0.05, respectively.[31] This result indicates that the solvent concentration around the PS segments in the PS/toluene solution is higher than that in the PS/DOP solution. This is quite reasonable because toluene and DOP are good and theta solvents for PS, respectively. In the dilute PS/toluene solution, the intermolecular hindrances on the segmental dynamics are expected to be small because of the high local concentration of mobile toluene. As mentioned above, we cited lesser intermolecular hindrances around chain ends as the origin of the higher mobility of chain ends in the bulky polymer liquid. However, in the dilute solution, these hindrances will be small even for the midchain segments. Therefore, we consider that the chain end segments no longer show distinctly higher mobility when the midchain segments are plasticized enough by the addition of mobile solvents. Even when the concentration of the PS increased to 60 wt %, the E-PS showed the same mobility with the M-PS within experimental uncertainties. If the PS concentration is increased more, E-PS would show higher mobility than the M-PS; however, the homogeneous solution with high PS concentration is hard to be prepared.

On the other hand, the E-PS showed slightly higher mobility compared to the M-PS in the concentrated PS/DOP (50/50) solution. DOP is a theta solvent of PS; therefore, the high value of the ϕ_{self} was determined by Lutz et al.[31] In the concentrated PS/DOP (50/50) solution, the local concentration of DOP around the PS segments is low. Moreover, the DOP is a remarkably viscous solvent. In this solution, the segmental motion of PS is expected to be restricted by the intermolecular hindrances although the restrictions are smaller than those in the bulk PS. Therefore, we considered that the chain ends showed slightly higher mobility than midchain segments because lesser intermolecular hindrances around chain ends were distinct in this viscous solution as well as in the bulk PS.

One may wonder that the chain ends should have higher mobility even in dilute solutions because the steric hindrance at the chain end is smaller than those at midchain segments. We do not negate this idea. If the measurement is sensitive to very local motion such as a rotation of only one C−C bond, higher mobility at the chain end could be detected even in dilute solutions. However, the spin-label method seems to insensitive to such very local motion of a polymer.[13−16] Recently, Kajiwara detected ESR spectra of propagation radicals of poly(*tert*-butyl methacrylate) whose molecular weight was controlled by atom transfer radical polymerization.[40] In this method, the polymer is essentially nonlabeled; the ESR spectrum is sensitive for the rotation at terminal $C_\alpha-C_\beta$ bond. Kajiwara showed the molecular weight dependence on the rotation at this bond in the solution. This method may reveal further unique characters of chain end motion of polymers.

Comparison to Other Techniques on Chain End Motion. The spin-labeling is perhaps the most popular technique to determine the chain end mobility of polymers in dilute solutions.[8−12] In particular, Bullock et al. and Yang et al. determined the chain end mobility of spin-labeled PS in dilute solutions with toluene and THF, respectively.[9,10] In these studies, the terminal of the PS main chain was spin-labeled with *tert*-butyl nitroxide. On the other hand, the para position of a phenyl ring of PS was randomly labeled with *tert*-butyl nitroxide as a reference sample; the mobility of these samples was analyzed from the line width of the ESR spectra. At 298 K, the correlation time for the end-labeled PS in toluene was about 2.4×10^{-10} s, whereas that for the PS labeled at the phenyl ring was about 5.9×10^{-10} s. It was claimed that the chain end of PS had higher mobility in the dilute solutions. Our result presented in this paper disagreed with Bullock's and Yang's results because the E-PS and M-PS showed the same mobility within experimental uncertainties in the dilute PS/toluene solution. As Pilař described in his literature, the line width cannot be fully and unambiguously related to the nitroxide rotational parameters without additional assumptions about the motion.[28] Moreover, the motional correlation times determined in Bullock's and Yang's studies are including a contribution of the rotation at polymer−label bond; the rotational rates for the end-labeling and ring-labeling might be different. Perhaps, the end-labeled PS showed higher mobility than the ring-labeled PS in the dilute solutions because of the difference in the rotational rate at the polymer−label bond for these samples or the ambiguity in the line-width analysis. The spin-label unit used for the M-PS and E-PS was the same and mobility was determined from the ESR line-shape analysis in the present work.

Horinaka et al. compared the mobility of the chain end and the center of the PS main chain using the fluorescence depolarization method from 283 to 303 K.[5] The segmental correlation time is determined from monitoring the anthracene reorientation which is covalently bonded into the center or chain end of the chain backbone. The internal rotation of

the anthracene in the backbone does not contribute to the reorientational relaxation of the transition moment. As the molecular weight of the PS was more than 2 kDa, the correlation time for the end-labeled PS in benzene at 293 K was about 3.0×10^{-10} s, whereas that for the center chain one was about 2.0×10^{-9} s. They concluded that the conformational transition at the chain end occurs easily compared to the center of the chain. We agree with that the rotation at the terminal C−C bond is easier than those of the inner C−C bonds due to the smaller steric hindrance at the chain end; therefore, if the measurement is sensitive to very local motion such as the rotation of only the terminal C−C bond, higher mobility at the chain end may be shown even in the dilute solution because very local motion is expected to be insensitive to the local concentration. However, as mentioned above, the bulky anthracene chromophore makes the PS segment rigid and the length scale of the segmental motion detected by the fluorescence measurement is expected to be somewhat larger than that in the NMR and ESR measurements. In fact, the center-anthracene-labeled PS showed slower mobility compared to the ESR and NMR data (Figure 6). On the other hand, the end-anthracene-labeled PS showed higher mobility than the ESR and NMR data. When the anthracene is bonded at the chain terminal, the rigidity given to the polymer segment could be smaller compared to the case of that the anthracene is bonded at the chain center. Therefore, we speculate a possibility of the lesser disturbance of the anthracene-labeling at the chain end on the segmental dynamics of PS.

To our knowledge, the segmental dynamics at the chain end of PS in the bulky liquid was studied only by Lund et al. using dielectric spectroscopy except to our ESR study.[7] Lund et al. synthesized end-functionalized oligomer PS (PS−Si-$(CH_3)_2(CH_2)_3$−CN; M_n = 2.2 kDa) to determined the chain end mobility of PS in the bulk over an extensive temperature range (ca. 50−413 K) using dielectric spectroscopy. Although the direct comparison of the absolute values of the relaxation rates determined by the dielectric and ESR measurements are impossible because the M_n of PS and the measurement temperature are different in these measurements, both measurements showed qualitative agreement of that the chain ends showed higher mobility compared to the midchain segments in the bulk.

The mobility of chain ends seems to depend on measurement methods because each method might detect different length scales of polymer chain motion; furthermore, labeling methods could disturb the original mobility of a polymer chain. Therefore, we propose that further various experiments including nonlabel methods are necessary to reveal unique characteristics of polymer chain ends.

Conclusion

Influences of solvents on the segmental dynamics at the chain end of PS have been investigated using the site-specific spin-label technique of ESR. The E-PS showed obviously and slightly higher mobility compared to the M-PS in the bulk PS and in the concentrated PS/DOP (50/50) solution, respectively. In these conditions, intermolecular hindrances for the segmental motion are large because of the high local concentration of PS. However, lesser intermolecular hindrances around chain ends are expected due to the large specific free volume around chain ends; this was proposed as the origin of the higher segmental mobility at the chain end. On the other hand, the E-PS showed the same mobility with the M-PS within experimental uncertainties in the dilute PS/toluene (1/99), concentrated PS/toluene (60/40), and dilute PS/DOP (3/97) solutions. We considered that the intermolecular hindrances were reduced and PS segments were plasticized enough by the solvents in these solutions; therefore, the chain ends no longer showed distinctly higher mobility than other segments. As a conclusion of this study, lesser intermolecular hindrances around chain ends are proposed as the origin of the higher segmental mobility at the chain end.

References and Notes

(1) Fox, T. G.; Flory, P. J. *J. Appl. Phys.* **1950**, *21*, 581–591.
(2) Fox, T. G.; Flory, P. J. *J. Polym. Sci.* **1954**, *14*, 315–319.
(3) Kajiyama, T.; Tanaka, K.; Takahara, A. *Macromolecules* **1997**, *30*, 280–285.
(4) Yu, W.; Sung, C. S. P.; Robertson, R. E. *Macromolecules* **1988**, *21*, 355–364.
(5) Horinaka, J.; Maruta, M.; Ito, S.; Yamamoto, M. *Macromolecules* **1999**, *32*, 1134–1139.
(6) Welp, K. A.; Wool, R. P.; Agrawal, G.; Satija, S. K.; Pispas, S.; Mays, J. *Macromolecules* **1999**, *32*, 5127–5138.
(7) Lund, R.; Plaza-García, S.; Alegría, A.; Colmenero, J.; Janoski, J.; Chowdhuny, S. R.; Quirk, R. P. *Macromolecules* **2009**, *42*, 8875–8881.
(8) Bullock, A. T.; Cameron, G. G.; Krajewski, V. *J. Phys. Chem.* **1976**, *80*, 1792–1797.
(9) Bullock, A. T.; Cameron, G. G.; Reddy, N. K. *J. Chem. Soc., Faraday Trans. 1* **1978**, *74*, 727–732.
(10) Yang, H. W. H.; Chien, J. C. W. *Macromolecules* **1978**, *11*, 759–763.
(11) Friedrich, C.; Lauprêre, F.; Noël, C.; Monnerie, L. *Macromolecules* **1981**, *14*, 1119–1125.
(12) Pilař, J.; Labsky, J. *J. Phys. Chem.* **1986**, *90*, 6038–6044.
(13) Miwa, Y.; Tanase, T.; Yamamoto, K.; Sakaguchi, M.; Sakai, M.; Shimada, S. *Macromolecules* **2003**, *36*, 3235–3239.
(14) Miwa, Y.; Yamamoto, K.; Sakaguchi, M.; Sakai, M.; Makita, S.; Shimada, S. *Macromolecules* **2005**, *38*, 832–838.
(15) Miwa, Y.; Sugino, Y.; Yamamoto, K.; Tanabe, T.; Sakaguchi, M.; Sakai, M.; Shimada, S. *Macromolecules* **2004**, *37*, 6061–6068.
(16) Miwa, Y.; Tanabe, T.; Yamamoto, K.; Sugino, Y.; Sakaguchi, M.; Sakai, M.; Shimada, S. *Macromolecules* **2004**, *37*, 8612–8617.
(17) Jeschke, G.; Schlick, S. In Schlick, S., Ed.; *Advanced ESR Methods in Polymer Research*; Wiley: Hoboken, NJ, 2006; Chapter 1, pp 3−24.
(18) Miwa, Y. *Macromolecules* **2009**, *42*, 6141–6146.
(19) Adam, G.; Gibbs, J. H. *J. Chem. Phys.* **1965**, *43*, 139–146.
(20) Rizos, A. K.; Ngai, K. L. *Macromolecules* **1998**, *31*, 6217–6225.
(21) Li, H.; Ujihira, Y.; Nanasawa, A. *Kobunshi Ronbunshu* **1996**, *53*, 358–365.
(22) Richardson, M. J.; Savill, N. G. *Polymer* **1977**, *18*, 3–9.
(23) Berry, G. C. *J. Chem. Phys.* **1967**, *46*, 1338–1352.
(24) Schneider, D. J.; Freed, J. H. In *Biological Magnetic Resonance*; Berliner, L. J., Reuben, J., Eds.; Plenum: New York, 1989; Vol. *8*, Chapter 1, pp 1−76.
(25) Miwa, Y.; Drews, A. R.; Schlick, S. *Macromolecules* **2008**, *41*, 4701–4708.
(26) Budil, D. E.; Lee, S.; Saxena, S.; Freed, J. H. *J. Magn. Reson., Ser. A* **1996**, *120*, 155–189.
(27) (a) Meirovitch, E.; Nayeem, A.; Freed, J. H. *J. Phys. Chem.* **1984**, *88*, 3454–3465. (b) Xu, D.; Budil, D. E.; Ober, C. K.; Freed, J. H. *J. Phys. Chem.* **1996**, *100*, 15867–15872. (c) Liang, Z.; Freed, J. H. *J. Phys. Chem. B* **1999**, *103*, 6384–6396. (d) Earle, K. A.; Budil, D. E. In Schlick, S., Ed.; *Advanced ESR Methods in Polymer Research*; Wiley: Hoboken, NJ, 2006; Chapter 3, pp 53−83.
(28) Pilař, J. In Schlick, S., Ed.; *Advanced ESR Methods in Polymer Research*; Wiley: Hoboken, NJ, 2006; Chapter 6, pp 133−163, and references therein.
(29) Capiomont, A. *Acta Crystallogr., Sect. B* **1972**, *28*, 2298–2301.
(30) He, Y.; Lutz, T. R.; Ediger, M. D.; Ayyagari, C.; Bedrov, D.; Smith, G. D. *Macromolecules* **2004**, *37*, 5032–5039.
(31) Lutz, T. R.; He, Y.; Ediger, M. D. *Macromolecules* **2005**, *38*, 9826–9835.
(32) Waldow, D. A.; Ediger, M. D.; Yamaguchi, Y.; Matsushita, Y.; Noda, I. *Macromolecules* **1991**, *24*, 3147–3153.
(33) Zhu, W.; Ediger, M. D. *Macromolecules* **1997**, *30*, 1205–1210.
(34) Santangelo, P. G.; Roland, C. M. *Macromolecules* **1998**, *31*, 4581–4585.
(35) Roland, C. M.; Nagai, K. L. *Macromolecules* **1996**, *29*, 5747–5750.

(36) Rizos, A. K.; Ngai, K. L. *Macromolecules* **1998**, *31*, 6217–6225.
(37) Boyer, R. F. *Macromolecules* **1974**, *7*, 142–143.
(38) Cowie, J. M. G. *Eur. Polym. J.* **1975**, *11*, 297–300.
(39) Chung, G.-C.; Kornfield, J. A.; Smith, S. D. *Macromolecules* **1994**, *27*, 5729–5747.
(40) Lodge, T. P.; McLeish, T. C. B. *Macromolecules* **2000**, *33*, 5278–5284.
(41) Kajiwara, A. In Schlick, S., Ed.; *Advanced ESR Methods in Polymer Research*; Wiley: Hoboken, NJ, 2006; Chapter 5, pp 101−131.